Wave Motion 54 (2015) 1–10

Contents lists available at ScienceDirect

Wave Motion

journal homepage: www.elsevier.com/locate/wavemoti

Improved multimodal methods for the acoustic propagation in waveguides with finite wall impedance

Simon Félix [a,*], Agnès Maurel [b], Jean-François Mercier [c]

[a] LAUM, CNRS, Université du Maine, avenue Olivier Messiaen, 72085 Le Mans, France
[b] Institut Langevin, CNRS, ESPCI ParisTech, 1 rue Jussieu, 75005 Paris, France
[c] Poems, CNRS, ENSTA ParisTech, INRIA, 828 boulevard des Maréchaux, 91762 Palaiseau, France

HIGHLIGHTS

- We address the problem of acoustic propagation in waveguides with treated boundaries.
- Two improved multimodal formulations are proposed and compared.
- Both formulations significantly increase the convergence of the modal method.
- The formulation with a supplementary mode is found to be the most efficient.

ARTICLE INFO

Article history:
Received 9 November 2013
Received in revised form 18 November 2014
Accepted 19 November 2014
Available online 4 December 2014

Keywords:
Waveguides
Modal method
Robin condition
Boundary modes

ABSTRACT

We address the problem of acoustic propagation in waveguides with wall impedance, or Robin, boundary condition. Two improved multimodal methods are developed to remedy the problem of the low convergence of the series in the standard modal approach. In the first improved method, the series is enriched with an additional mode, which is thought to be able to restore the right boundary condition. The second improved method consists in a reformulation of the expansions able to restore the right boundary conditions for any truncation, similar to polynomial subtraction technique. Surprisingly, the first improved method is found to be the most efficient. Notably, the convergence of the scattering properties is increased from N^{-1} in the standard modal method to N^{-3} in the reformulation and N^{-5} in the formulation with a supplementary mode. The improved methods are shown to be of particular interest when surface waves are generated near the impedance wall.

1. Introduction

We address the problem of acoustic wave propagation problem, $(\Delta + k^2)p(x, y) = 0$, within a waveguide with, locally, an impedance boundary condition at the wall ($y = h$):

$$\partial_y p(x, h) = \frac{1}{Z(x)} p(x, h), \quad x \in [0, L] \tag{1}$$

with $Z(x)$ the surface impedance (Fig. 1). This impedance condition, also referred as Robin condition [1–5], is of practical interest, since it describes non perfectly reflecting surfaces or absorbing materials at a waveguide wall. Limiting cases are the Neumann boundary condition $Z = \infty$ and the Dirichlet boundary condition $Z = 0$.

* Corresponding author.
E-mail address: simon.felix@univ-lemans.fr (S. Félix).

http://dx.doi.org/10.1016/j.wavemoti.2014.11.007
0165-2125/

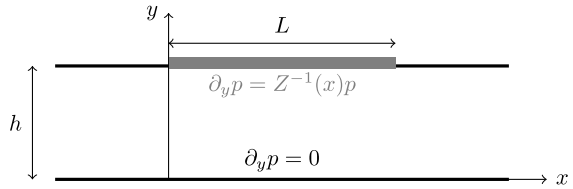

Fig. 1. Waveguide with the upper wall submitted to a localized Robin boundary condition ($0 \leq x \leq L$), Neumann boundary condition otherwise.

Table 1
Convergences of the remaining series, of the scattering coefficients and of the scattered field in the standard multimodal formulation (SMF), in the reformulation (RF) and in the formulation with a supplementary mode (SupMF).

	Standard modal formulation	Reformulation	Supplementary mode
Remaining series	$1/N^{1.5}$	$1/N^{3.5}$	$1/N^{3.5}$
Error on the scattering coef.	$1/N$	$1/N^3$	$1/N^5$
Error on the scattered field	$1/N$	$1/N^3$	$1/N^{3.5}$

Classically, that is, in waveguides with rigid boundaries, multimodal formulations involve the expansion of the solution on the *rigid* transverse modes $\varphi_n(y)$ satisfying the Neumann boundary condition:

$$p(x,y) = \sum_{n=0}^{N} p_n(x)\varphi_n(y). \tag{2}$$

Since the infinite set of $\varphi_n, N \to \infty$, is a complete basis, the decomposition is still valid in segments with Robin boundary condition at the walls, as done in [6,7]. However, because the boundary condition is not satisfied by the transverse modes, the series has poor convergence, attributable in part to the non uniform convergence of the pressure derivative. This results in the appearance of Gibbs oscillations close to the treated wall. In the case of waveguides with varying cross-section, it has been shown in Refs. [8–11] that this situation can be remedied by adding to the usual expansion an additional term (called supplementary mode in the sequel):

$$p(x,y) = \sum_{n=0}^{N-1} p_n(x)\varphi_n(y) + p_{-1}(x)\varphi_{-1}(y), \tag{3}$$

where φ_{-1} is chosen such that $\varphi'_{-1}(h) \neq 0$ (note that this ensures that φ_{-1} is not a finite combination of the $\{\varphi_n\}_{n\geq 0}$, otherwise φ_{-1} would be trivially absorbed into the φ_n-series above a given order). In this approach, it is thought that the supplementary mode will be able to restore the right boundary condition if $Z(x)p_{-1}(x)\varphi'_{-1}(h) = p(x,h)$. However, this is not guaranteed *a priori*; in the case of waveguides with varying cross section, it has been shown that the right boundary condition is restored only asymptotically, for $N \to \infty$ [9].

Alternatively to this supplementary mode, Bi et al. [12] proposed a reformulation of the modal expansion that restores the exact boundary condition for any truncation of the series. Instead of using an additional unknown $p_{-1}(x)$, the projection is written

$$p(x,y) = \sum_{n=0}^{N} p_n(x)[\varphi_n(y) + Y(x)\varphi_n(h)\xi(y)] \tag{4}$$

with $Y(x) = Z^{-1}(x)$ the surface admittance. With $\xi(y)$ being chosen such as $\xi(h) = 0$ and $\xi'(h) = 1$, it is easy to see that the condition $\partial_y p(x,h) = Y(x)p(x,h)$ is satisfied for any N value. Finally, the function $\xi(y)$ is chosen in order to ensure that the truncated series satisfies the Neumann boundary condition at $y = 0$, thus such that $\xi'(0) = 0$. This reformulation is similar to the so-called polynomial subtraction method [13–15] (see also [9,10] for a discussion in the 2D-case).

Note that, in Eqs. (2) and (3), the p_n-functions correspond to the usual modal components $p_n = (p, \varphi_n)$, with (f, g) the scalar product $\int_0^h \mathrm{d}y\ f(y)\overline{g}(y)$. However, in Eq. (4), they are defined as the modal component of a related field $\tilde{p}$ ($p_n \equiv \left(\tilde{p}, \varphi_n\right)$), with $\tilde{p}(x,y) \equiv p(x,y) - Y(x)p(x,h)\xi(y)$ (see Section 2.2).

In this paper, we compare the two improved multimodal approaches. As expected, both formulations lead to an increased convergence. However, one may think that the expansion proposed in the reformulation, Eq. (4), that exactly satisfies the boundary condition (1), is the most efficient because it ensures the uniform convergence of the derivative of the series. In fact, both formulations give similar convergence rate and accuracy for the wavefield in the scattering region. More surprisingly, when computing the scattering coefficients, the "supplementary mode" formulation (SupMF) is characterized by a superconvergence: while the standard modal expansion converges as $1/N$ and the reformulation (4) as $1/N^3$, it indeed displays a $1/N^5$ convergence rate. Summarized convergence properties are presented in Table 1.

The paper is organized as follows. In Section 2, the multimodal formulations issued from the expansions in Eqs. (2)–(4) are derived. Results on the convergence are presented in Section 3. Technical calculations are collected in the appendices.

2. Multimodal formulations

In this section, we use the modal expansion in the three formulations (2)–(4) to derive the corresponding systems of coupled mode equations. The calculations are presented in the two dimensional case; the elements needed to treat the axisymmetric three dimensional case are collected in Appendices A and B.

First, we define an intermediate field $q(x, y)$ (basically, the velocity component along the x-axis) and rewrite the Helmholtz equation

$$\begin{cases} q(x,y) \equiv \dfrac{\partial p}{\partial x}(x,y), \\ \dfrac{\partial q}{\partial x}(x,y) = -\dfrac{\partial^2 p}{\partial y^2}(x,y) - k^2 p(x,y), \end{cases} \tag{5}$$

with boundary conditions $\partial_y p(x, 0) = 0$ and $\partial_y p(x, h) = Y(x)p(x, h)$. Next, the two fields p and q will be expanded onto N functions chosen – differently – in each formulation, and the above equations will be projected using the scalar product $(f, g) \equiv \int_0^h \mathrm{d}y\, f(y)\overline{g}(y)$.

2.1. The standard multimodal formulation (SMF)

In the usual formulation, p and q are simply expanded onto the set of the first N rigid transverse eigenfunctions $\varphi_n(y)$ ($N \geq N_\mathrm{p}$, N_p the number of propagative modes):

$$\begin{cases} p(x,y) = \displaystyle\sum_{n=0}^{N-1} p_n(x)\varphi_n(y), \\ q(x,y) = \displaystyle\sum_{n=0}^{N-1} q_n(x)\varphi_n(y), \end{cases} \tag{6}$$

and the $\varphi_n(y)$ are, in two dimensions,

$$\varphi_n(y) = \sqrt{\frac{2-\delta_{n0}}{h}}\cos\frac{n\pi y}{h}. \tag{7}$$

To project Eqs. (5) with the expansions in Eqs. (6), we use that the series can be derived ones term by term, since φ_n forms a basis of $H^1(]0, h[)$ (in $L^2(]0, h[)$ with derivative in $L^2(]0, h[)$ [16]). However, the second equation in (5) involves a second derivative, so that we use the integration by part

$$\int_0^h \mathrm{d}y\, \frac{\partial^2 p}{\partial y^2}(x,y)\varphi_n(y) = -\int_0^h \mathrm{d}y\, \frac{\partial p}{\partial y}(x,y)\varphi_n'(y) + Y(x)p(x,h)\varphi_n(h), \tag{8}$$

to get the projection of the second derivative of p

$$\left(\frac{\partial^2 p}{\partial y^2}, \varphi_n\right) = -\gamma_n^2 p_n(x) + Y(x)\varphi_m(h)\varphi_n(h)p_m(x), \tag{9}$$

where we have also used $\left(\varphi_m', \varphi_n'\right) = \gamma_n^2\delta_{mn}$, with

$$\gamma_n \equiv (n\pi/h). \tag{10}$$

Note that in Eq. (9), and throughout the paper, the absence of sum symbols means that the Einstein summation convention has been used.

The other series are derived term by term and the projections of Eqs. (5) lead to

$$\begin{cases} p_n' = q_n, \\ q_n' = \left[-k_n^2\delta_{mn} - Y(x)\varphi_n(h)\varphi_m(h)\right]p_m, \end{cases} \tag{11}$$

which can be written in a matrix form

$$\begin{pmatrix} \mathbf{p} \\ \mathbf{q} \end{pmatrix}' = \begin{pmatrix} 0 & \mathsf{I} \\ \mathsf{K}^2 - Y(x)\mathsf{D} & 0 \end{pmatrix}\begin{pmatrix} \mathbf{p} \\ \mathbf{q} \end{pmatrix} \tag{12}$$

with $K_{mn} \equiv ik_n\delta_{mn}$, $k_n^2 = k^2 - \gamma_n^2$, and $\mathsf{D}_{mn} \equiv \varphi_m(h)\varphi_n(h)$ (see Appendix B).

2.2. A natural reformulation (RF)

The basic idea of the RF is to identify a field that satisfies Neumann boundary conditions at $y = 0$ and $y = h$. This field will be then expanded on the $\varphi_n(y)$ safely, that is, expecting a good convergence. It is easy to check that

$$\tilde{p}(x,y) \equiv p(x,y) - Y(x)p(x,h)\xi(y) \tag{13}$$

satisfies $\partial_y \tilde{p}(x,h) = 0$ if $\xi(y)$ is chosen to satisfy $\xi'(h) = 1$. Next, it is convenient to choose $\xi(h) = 0$ in order to express simply p as a function of the modal components of $\tilde{p}$

$$\tilde{p}(x,y) = \sum_{n=0}^{N-1} p_n(x)\varphi_n. \tag{14}$$

Indeed, with $\xi(h) = 0$, we have $p(x,h) = \tilde{p}(x,h)$, from which we deduce $p(x,y) = \tilde{p}(x,y) + Y(x)\tilde{p}(x,h)\xi(y)$, and we finally get a modified form of the expansion for p (the same expansion for q than in Eqs. (6) is chosen)

$$\begin{cases} p(x,y) = \displaystyle\sum_{n=0}^{N-1} p_n(x)\left[\varphi_n(y) + Y(x)\varphi_n(h)\xi(y)\right], \\ q(x,y) = \displaystyle\sum_{n} q_n(x)\varphi_n(y). \end{cases} \tag{15}$$

We choose a function ξ which satisfies both constraints $\xi'(h) = 0$ and $\xi(h) = 0$

$$\xi(y) \equiv -\frac{2h}{\pi}\cos\left(\frac{\pi y}{2h}\right) \tag{16}$$

(note that other choices can be done). The projections of the two equations in Eq. (5) are straightforward, using Eqs. (15); we get

$$\begin{cases} q_n = \left[\delta_{mn} + Y(x)\varphi_m(h)\xi_n\right] p'_m + Y'(x)\varphi_m(h)\xi_n p_m, \\ q'_n = \left[-k_n^2\left(\delta_{mn} + Y(x)\varphi_m(h)\xi_n\right) - Y(x)\varphi_m(h)\varphi_n(h)\right] p_m, \end{cases} \tag{17}$$

with $\xi_n \equiv (\xi, \varphi_n)$. Defining the matrices $\mathsf{E} \equiv \mathsf{I} + Y(x)\mathsf{C}$ and $\mathsf{C}_{nm} \equiv \xi_n\varphi_m(h)$ (see Appendix B), we get a new coupled mode system

$$\begin{pmatrix} \mathbf{p} \\ \mathbf{q} \end{pmatrix}' = \begin{pmatrix} -Y'(x)\mathsf{E}^{-1}\mathsf{C} & \mathsf{E}^{-1} \\ \mathsf{K}^2\mathsf{E} - Y(x)\mathsf{D} & 0 \end{pmatrix} \begin{pmatrix} \mathbf{p} \\ \mathbf{q} \end{pmatrix}. \tag{18}$$

For piecewise constant impedance, the system reduces to

$$\mathsf{E}\mathbf{p}'' = (\mathsf{K}^2\mathsf{E} - Y\mathsf{D})\mathbf{p}, \tag{19}$$

in agreement with Ref. [7], where the calculations are performed in the three dimensional case (see Eq. (24) with Eqs. (23) and (25) in this reference).

2.3. The supplementary mode formulation (SupMF)

We adapt the method considered in [8,9] for waveguides with varying cross section. The idea is to enrich the usual expansion with a mode whose derivative does not vanish at $y = h$. Contrary to the RF, this supplementary mode being an additional unknown, it is not guaranteed that the right boundary condition is verified at the wall with Robin boundary condition.

The supplementary mode is associated to an additional transverse function $\varphi_{-1}(y)$. This function is built to be orthogonal to the N first rigid eigenfunctions φ_n, $0 \le n \le (N-2)$ namely,

$$\begin{cases} \varphi_{-1}(y) \equiv a_{-1}\left[\chi(y) - \displaystyle\sum_{n=0}^{N-2}\chi_n\varphi_n(y)\right], \\ \chi(y) \equiv \sqrt{\dfrac{2}{h}}\cos\dfrac{\pi y}{2h}, \end{cases} \tag{20}$$

where we have defined $\chi_n \equiv (\chi, \varphi_n)$ and where a_{-1} is a normalization factor of φ_{-1} ($\|\varphi_{-1}\| = 1$). Finally, the mode φ_{-1} satisfies the relation $\left(\varphi'_{-1}, \varphi'_n\right) = \gamma_{-1}\delta_{-1,n}$ with

$$a_{-1}^2 = \frac{1}{1 - \displaystyle\sum_{n=0}^{N-2}\chi_n^2}, \qquad \gamma_{-1}^2 = \frac{\|\chi'\|^2 - \displaystyle\sum_{n=0}^{N-2}\chi_n^2\gamma_n^2}{1 - \displaystyle\sum_{n=0}^{N-2}\chi_n^2}. \tag{21}$$

Note that both a_{-1} and γ_{-1} depend on the truncation N. It is easy to see that the new expansions

$$\begin{cases} p(x,y) = \displaystyle\sum_{n=-1}^{N-2} p_n(x)\varphi_n(y), \\ q(x,y) = \displaystyle\sum_{n=-1}^{N-2} q_n(x)\varphi_n(y), \end{cases} \tag{22}$$

have exactly the same structure and properties as the standard modal expansion Eq. (6), with $-1 \leq n, m \leq (N-2)$. It follows that the projection of the Helmholtz equation with the boundary conditions leads to the same matrix expression Eq. (12) as in the SMF. Besides, it has been shown in [9] that the supplementary mode behaves as an evanescent mode associated to a wavenumber $k_{-1}^2 = k^2 - \gamma_{-1}^2 < 0$. This is expected since the supplementary mode has to vanish far from the scattering region (only the propagative rigid modes exist in the far field). It is also easy to check that increasing the truncation N makes the supplementary mode more and more evanescent ($\gamma_{-1} \propto N$, see Eq. (2.12) of [9]). Finally, note that, in the limit $N \to \infty$, $\varphi_{-1} \to 0$ which is consistent since the usual rigid modes tend to form a complete basis.

2.4. Remarks on the modal systems

As a first remark, let us stress that the expansions of the solution in Eqs. (6), (15) and (22) do not satisfy the Helmholtz equation *a priori*. One has to derive the equations for the p_n components that make the expansion to satisfy it. This is done for each of the expansion (6), (15) and (22), leading to the system for the p_n (12) and (18) and (12) again.

Let us now consider the regularity of Y which is required in the different formulations. Obviously, the system Eq. (12) does not involve derivatives of $Y(x)$, so it can be used for discontinuous Y function (*e.g.*, a piecewise constant Y function as considered in [12]). On the contrary, the system (18) coming from the RF needs $Y(x)$ to be continuous. If not the case, one has to apply impedance matching technique but the convergence is expected to be lower. Besides, it is not obvious that real wall treatments are better described by discontinuous admittances since usual admittance models are obtained from a homogenization process. In the following section, we compare the three formulations in the case of a continuous Y function. The piecewise case is considered in Appendix C.

3. Results

The results presented in this section correspond to the two dimensional case. We have checked that similar behaviors are obtained in the three dimensional case. We consider a continuous $Y(x)$ function, namely

$$Y(x) = \begin{cases} Y_0 \sin^2(\pi x/2\delta) & \text{if } 0 \leq x \leq \delta, \\ Y_0 & \text{if } \delta < x < L-\delta, \\ Y_0 \sin^2(\pi (L-x)/2\delta) & \text{if } L-\delta \leq x \leq L, \end{cases} \tag{23}$$

with $Y_0 \in \mathbb{C}$. The parameter δ measures the transition length where the impedance goes from zero to Y_0 (and Y is symmetric with respect to $x = L/2$). The limit $\delta \to 0$ leads to a piecewise constant surface admittance and this case is discussed in Appendix C. The coupled mode systems are solved using a Möbius-Magnus scheme, as described in [6,17]. A plane wave $p^{(\text{inc})}(x, y) = e^{ikx}$ is sent from the left with frequency $kh = 0.2$ and we chose $L/h = 2$. The choice of a low frequency is made for the sake of clarity, without loss of generality. Indeed, at such frequencies – only one mode is propagating – the propagating field poorly describes the exact solution. The contribution of the additional modes to the total wavefield is thus highlighted, and therefore the differences between the three formulations are more visible. At higher frequency, the propagating field approximates reasonably the solution, making the effect of the additional modes less visible, though the relative difference between the formulations and their convergence are the same.

3.1. Results on the wavefield

A first check on the improved formulations is shown in Fig. 2. The behavior of the terms of the series in Eqs. (2)–(4) is reported; in the SMF and in the RF, the general term of the series is simply p_n. In the SupMF, the general term of the series is $P_n \equiv p_n - a_{-1}\chi_n p_{-1}$ because φ_{-1} also depends on the truncation number. As already observed in [7], the term p_n in the SMF varies as $1/n^2$ and as $1/n^4$ in the RF. The term P_n varies also as $1/n^4$ and this behavior has been observed in the case of waveguides with varying cross section [9]. These behaviors indicate that the error of the remaining series, $\sum_{n=N}^{+\infty} p_n\varphi_n$, is higher in the SMF ($1/N^{3/2}$) than in the two improved formulations ($1/N^{7/2}$).

Fig. 3 shows the wavefields calculated at a given N value ($N = 8$ and $Y_0 h = 10 + 10i$, $\delta/h = 0.1$; practically, in the SupMF, the summation is made from $n = -1$ to $N-2$, so that the number of degrees of freedom, N, is the same in each formulation). The relative deviations between these fields and the converged field (integrated over the whole domain) are: 4% in the SMF, 0.15% in the RF and 0.06% for the SupMF. Next, varying N, we observe the following convergences: $1/N$ for the SMF, $1/N^3$ for the RF, and $1/N^{7/2}$ for the SupMF (results are not reported). Note that these convergence rates of the SMF and RF are lower than the highest expected convergences, which are $1/N^{3/2}$ and $1/N^{7/2}$, respectively, and which are attributable to the behaviors of remaining series. Similar observations have been reported in the case of varying cross-section waveguides [9,10].

Fig. 4 shows the wavefields in a more involved case; With $Y_0 h = 10$, a surface wave takes place near $y = h$, associated to a typical length $\sim 2\pi/Y_0$. To obtain this result, it is sufficient to look for a solution $p(x, y) \propto e^{iKx-\sigma(h-y)}$ satisfying the dispersion relation and the boundary condition on the treated part of the wall (see also [18]). In this case, the error when using the SMF is high (around 40% whatever the N value is) and the field is still not converged at $N = 50$. The improved formulations have much smaller errors: in the RF 27% for $N = 8$, 6% for $N = 11$ and 0.8% for $N = 20$. In the SupMF: 1% for $N = 8$, 0.3% for $N = 11$ and less than 0.1% for $N = 20$. Although the rate of convergence of the scattered fields is merely

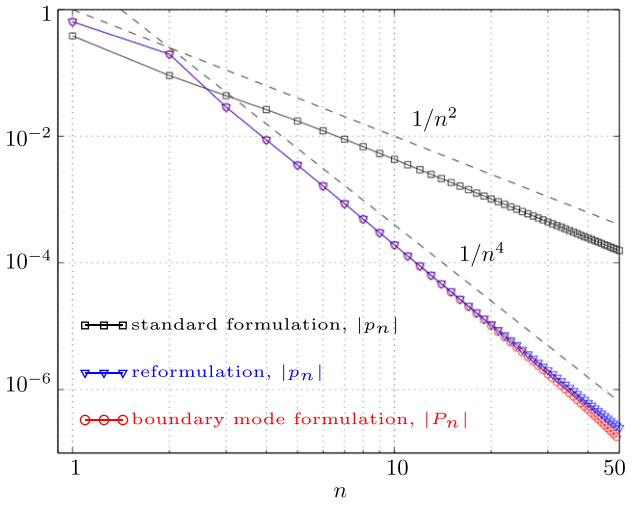

Fig. 2. Amplitude of the modal coefficients in the series (2)–(4) for the case displayed in Fig. 3.

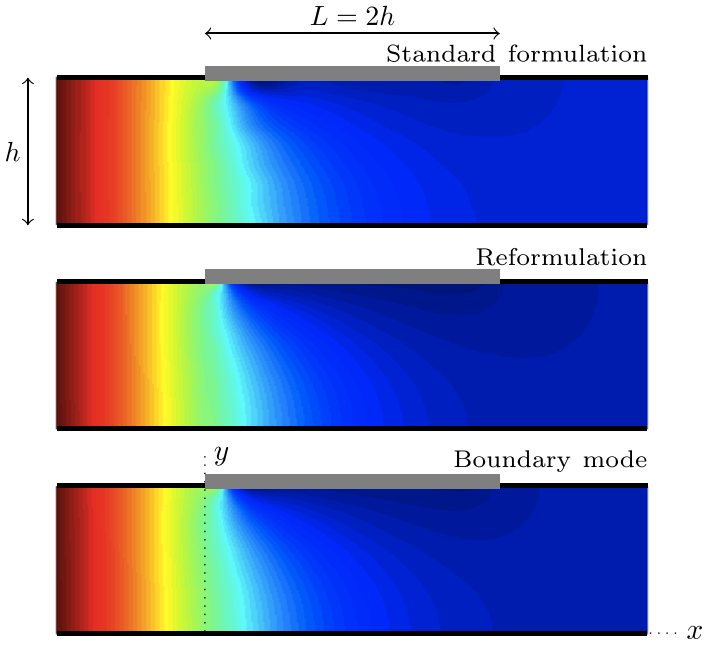

Fig. 3. Wavefield (real part) in the waveguide, at frequency $kh = 0.2$, with $Y(x)$ given by Eq. (23) and $Y_0h = 10 + 10i$, $\delta/h = h$ and $L/h = 2$. The field is plotted for $-h \le x \le 3h$. Calculations have been done with $N = 8$.

the same in the two improved formulations (namely $1/N^3$ and $1/N^{3.5}$), it appears that the initial value of the error (say, for small N) is higher in the RF than in the SupMF.

3.2. Results on the scattering coefficients

In this section, the convergence of the scattering coefficients R and T is examined. At low frequency – only the plane wave mode is propagating – and far enough from the scattering region, the field $p(x, y)$ reduces to

$$\begin{cases} p(x \le 0) = e^{ikx} + Re^{-ikx}, \\ p(x \ge L) = Te^{ikx}. \end{cases} \tag{24}$$

The convergence of R is shown in Fig. 5 for $Y_0h = 10$ and $Y_0h = 10 + 10i$ (otherwise, $\delta/h = 0.1$, $L/h = 2$ and $kh = 0.2$). It appears that the increase in the accuracy of the scattering coefficients is twofold. First, the rate of convergence is improved: from $1/N$ in the SMF to $1/N^3$ in the RF and to $1/N^5$ in the SupMF. Next, a more subtle effect is due to the transitory that

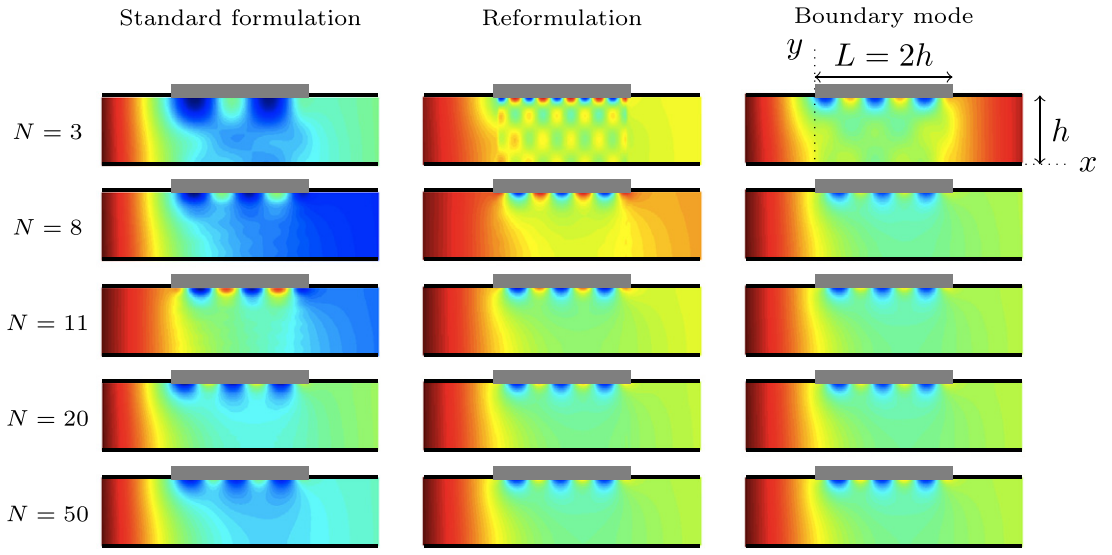

Fig. 4. Wavefield (real part) in the waveguide, at frequency $kh = 0.2$, with $Y(x)$ given by Eq. (23) and $Y_0h = 10$, $\delta/h = 0.1$ and $L/h = 2$. The field is plotted for $-h \leq x \leq 3h$.

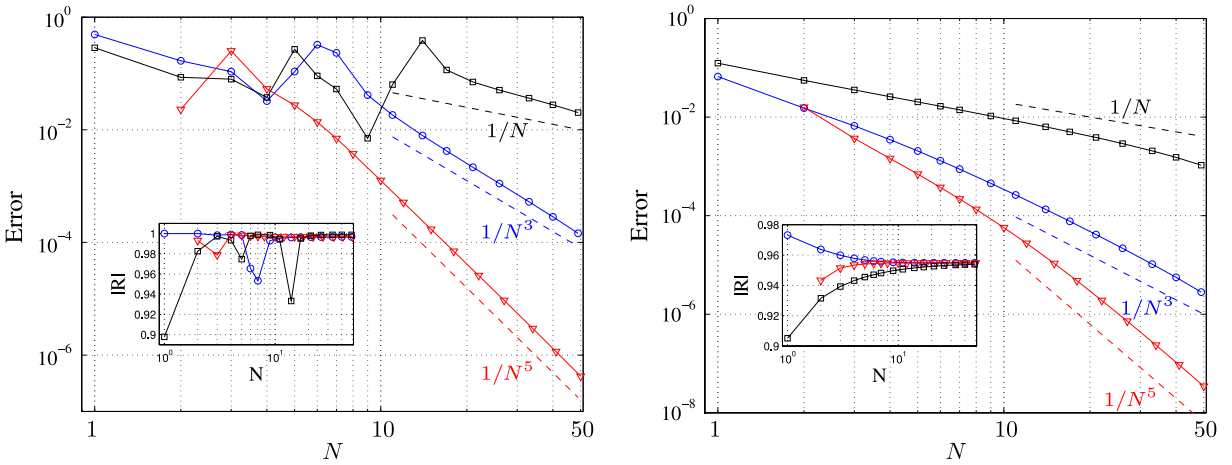

(a) $Y_0h = 10$. (b) $Y_0h = 10 + 10i$.

Fig. 5. Error on the reflection coefficient, as a function of the truncation N. Black squares: SMF; blue circles: RF; red triangles: SupMF. Insets show the corresponding reflection coefficient, as a function of N. The wall admittance $Y(x)$ is given by Eq. (23) with (a) $Y_0h = 10$ and (b) $Y_0h = 10 + 10i$. Otherwise, $\delta/h = 0.1$, $L/h = 2$, and $kh = 0.2$.

exists before the error enters in these power law behaviors: the improved formulations enter earlier in their power law behaviors than the SMF. Again, regarding this effect, the SupMF is more efficient than the RF, being almost not affected by the transitory.

Incidentally, we have also observed (results are not reported) that the size of the transitory is reduced (i) for smaller real part of Y_0 (this reduces the wavenumber of the surface mode), (ii) for higher imaginary part of Y_0 and (iii) for larger δ value.

The results on the observed convergences are collected in Table 1. Two convergences have to be regarded. The first convergence is given by the error on the remaining series $\sum_{n=N}^{\infty} p_n\varphi_n$, which corresponds to the error of truncation, that is usually considered. As previously said, this convergence directly follows from the convergence of the modal components p_n (Fig. 2); it is related to the uniform convergence (or non uniform convergence) of the solution. The second convergence is the convergence of the scattering coefficients. It is due to a convergence often disregarded. Indeed, the convergence of R and T is given by the convergence of the modal component $p_0(x)$ as N varies (since only mode 0 is propagating), and there is no theoretical results on the convergence of the coefficients p_n when N varies (see also [10,11]). As a result of the two previous convergences is the convergence for the scattered field. The latter includes the evanescent modes in the near field, and thus, it is limited by the lowest convergence of the two.

4. Conclusion

We have considered two modal methods that are able to improve the accuracy and the convergence of the standard multimodal formulation (SMF) for the problem of wave propagation in a waveguide with impedance boundary conditions at the walls. The improvement is particularly noticeable when surface waves are present near the treated wall, a situation that corresponds to non purely reactive wall impedances. Incidentally, regarding the previous studies [6,7,12], we have also generalized the problem to a varying wall admittance $Y(x)$.

As previously said, the reformulation (RF) restores the exact boundary condition at the lined wall for any truncation. The counterpart is that the mode perpendicular to the set of φ_n in Eq. (4) is a combination of the N rigid modes, similar to a slave mode in dynamical systems (namely, proportional to $Y(x)\sum\varphi_n(h)p_n(x)$). To the contrary, the formulation with a supplementary mode (SupMF) uses an additional unknown (a "master mode"), $p_{-1}(x)$ associated to $\varphi_{-1}(y)$. Notably, it is an evanescent mode associated to a purely imaginary wavenumber k_{-1} associated to the smallest resolved length (that is, smaller than any $1/|k_n|$). It turns out that these elements make the SupMF more efficient to describe the wavefield in the scattering region. Typically an accuracy of 1% is reached in the SupMF with only few modes while more than 10 modes are needed in the RF and while 100 modes in the SMF are not enough to reach such accuracy.

The improvement in the convergence of the scattering coefficients is even more remarkable: from $1/N$ in the SMF to $1/N^3$ in the RF and $1/N^5$ in the SupMF. The observed superconvergence is attributable to the convergence of the modal components of the propagating modes and there is still a lack of theoretical results on this type of convergence.

Acknowledgment

The authors acknowledge the financial support of the Agence Nationale de la Recherche through the grant ANR ProCoMedia, project ANR-10-INTB-0914.

Appendix A. The axisymmetric 3D case

Eq. (5) becomes, in the axisymmetric three dimensional case

$$\begin{cases} q(z,r) \equiv \dfrac{\partial p}{\partial z}(z,r), \\ \dfrac{\partial q}{\partial z}(z,r) = -\dfrac{1}{r}\dfrac{\partial}{\partial r}\left(r\dfrac{\partial p}{\partial r}\right) - k^2 p(z,r), \end{cases} \tag{A.1}$$

with boundary condition $1/r\ \partial_r p(z,R) = Y(z)p(z,R)$. The scalar product is defined by

$$(f,g) \equiv \int_0^R \mathrm{d}r\ rf(r)\overline{g}(r). \tag{A.2}$$

The projection of Eqs. (A.1) is done onto the transverse eigenfunctions

$$\varphi_n(r) = \frac{\sqrt{2}}{R}\frac{J_0(\gamma_n r)}{J_0(\gamma_n R)}, \tag{A.3}$$

where J_n denotes the nth order Bessel function of first kind, and with $\gamma_n R$ the zeros of J_1. The supplementary mode is defined by

$$\begin{cases} \varphi_{-1}(r) \equiv a_{-1}\left[\chi(r) - \displaystyle\sum_{n=0}^{N-1}\chi_n\varphi_n(r)\right], \\ \chi(r) \equiv \dfrac{\sqrt{2}}{R}\dfrac{J_0(\beta r)}{J_1(\beta R)}, \end{cases} \tag{A.4}$$

with βR a zero of J_0 (and we choose the first zero). Finally, the function $\xi(r)$ that can be used for the RF in Eq. (18) is

$$\xi(r) \equiv -\frac{J_0(\beta r)}{\beta J_1(\beta R)}. \tag{A.5}$$

Owing to these modifications, the modal system Eq. (12) for the SMF and for the SupMF remains the same and the modal system Eq. (18) for the RF remains the same.

Appendix B. Expressions of the matrices C and D

We give here the expressions of

$$\mathsf{C}_{nm} \equiv \xi_n\varphi_m(h), \quad \mathsf{D}_{nm} \equiv \varphi_n(h)\varphi_m(h)$$

(and h is replaced by R in the three dimensional case).

B.1. The two dimensional case

For the SMF, we need D only (symmetric) and it is sufficient to use

$$\begin{cases} \varphi_0(h) = 1/\sqrt{h}, \\ \varphi_n(h) = \sqrt{2/h}(-1)^n. \end{cases} \tag{B.1}$$

For the SupMF, we need $\varphi_{-1}(h) = -a_{-1}\sum_{n=0}^{N-1}\chi_n\varphi_n(h)$ in addition (and $a_{-1} = 1/\sqrt{1-\sum_{n=0}^{N-1}\chi_n^2}$). It is thus sufficient to have χ_n

$$\begin{cases} \chi_0 = \dfrac{2\sqrt{2}}{\pi}, \\ \chi_n = -\dfrac{4(-1)^{n+1}}{\pi(4n^2-1)}. \end{cases} \tag{B.2}$$

Finally, for the RF, C needs ξ_n, which can be simply deduced from χ_n using

$$\xi_n = -\frac{\sqrt{2}}{\pi}h^{3/2}\chi_n. \tag{B.3}$$

B.2. The three dimensional case

We have in this case

$$\varphi_n(R) = \frac{\sqrt{2}}{R}, \tag{B.4}$$

$$\chi_n = -\frac{-2\beta}{(\gamma_n^2-\beta^2)R}, \tag{B.5}$$

and

$$\xi_n = -\frac{R}{\sqrt{2}\beta}\chi_n. \tag{B.6}$$

Appendix C. The case of piecewise constant boundary impedance

The case of piecewise constant wall impedance $Y(x) = Y_0$ for $0 \le x \le L$ and zero outside this region cannot be treated with the modal system (18). Indeed in this case, the admittance matrix Y is discontinuous and the jumps at the discontinuities have to be calculated. To do that, we use

$$p(x,y) = \begin{cases} \displaystyle\sum_n p_n\psi_n(y), & x \in [0,L], \\ \displaystyle\sum_n p_n\varphi_n(y), & \text{otherwise}, \end{cases} \tag{C.1}$$

with $\psi_n(y) \equiv \varphi_n(y) + Y_0\varphi_n(h)\xi(y)$. Then, we use the continuity of p and $q = \partial_x p$ at $x = 0, L$, and project the relations $p(0^-,y) = p(0^+,y)$ and $q(0^-,y) = q(0^+,y)$ to get

$$\begin{cases} \mathbf{p}(0^-) = \mathsf{E}\mathbf{p}(0^+), \\ \mathbf{q}(0^-) = \mathsf{E}\mathbf{q}(0^+) \end{cases} \tag{C.2}$$

and the same at $x = L$ where E is evaluated in the admittance area ($\mathsf{E} \equiv \mathsf{I} + Y_0\mathsf{C}$). Although this model of a discontinuous $Y(x)$ is simple (when compared to our approach where Y goes from 0 to Y_0 within a boundary layer of size δ), the main disadvantage is that it produces a gradient of the wave field p singular at one point. The resulting convergence of the wavefield is thus reduced and we have observed the following behaviors: in the SMF, the scattering coefficients converges as $1/N$ as previously but the convergence in the improved formulations is only $1/N^2$.

References

[1] K. Gustafson, T. Abe, The third boundary condition - what is Robin's? Math. Intell. 20 (1998) 63–71.
[2] J.A. Roden, S.D. Gedney, The efficient implementation of the surface impedance boundary condition in general curvilinear coordinates, IEEE Trans. Microw. Theory Tech. 47 (1999) 1954–1963.
[3] H. Barucq, C. Bekkey, R. Djellouli, Construction of local boundary conditions for an eigenvalue problem using micro-local analysis: application to optical waveguide problems, J. Comput. Phys. 193 (2004) 666–696.

[4] I. Simonsen, A.A. Maradudin, T.A. Leskova, Scattering of electromagnetic waves from two-dimensional randomly rough penetrable surfaces, Phys. Rev. Lett. 104 (2010) 223904.
[5] O. Olendski, L. Mikhailovska, Theory of a curved planar waveguide with Robin boundary conditions, Phys. Rev. E 81 (2010) 036606.
[6] S. Félix, V. Pagneux, Sound attenuation in lined bends, J. Acoust. Soc. Am. 116 (2004) 1921–1931.
[7] W. Bi, V. Pagneux, D. Lafarge, Y. Aurégan, Modelling of sound propagation in a non-uniform lined duct using a multi-modal propagation method, J. Sound Vib. 289 (2006) 1091–1111.
[8] G.A. Athanassoulis, K.A. Belibassakis, A consistent coupled-mode theory for the propagation of small-amplitude water waves over variable bathymetry regions, J. Fluid Mech. 389 (1999) 275–301.
[9] J.-F. Mercier, A. Maurel, Acoustic propagation in non uniform waveguides: revisiting Webster equation using evanescent boundary modes, Proc. R. Soc. A 469 (2013) 20130186.
[10] A. Maurel, J.-F. Mercier, V. Pagneux, Improved multimodal admittance method in varying cross section waveguide, Proc. R. Soc. A 470 (2014) 20130448.
[11] A. Maurel, J.-F. Mercier, S. Félix, Propagation in waveguides with varying cross-section and curvature: A new light on the role of supplementary modes in multimodal methods, Proc. R. Soc. A 470 (2014) 20140008.
[12] W. Bi, V. Pagneux, D. Lafarge, Y. Aurégan, An improved multimodal method for sound propagation in non uniforms lined ducts, J. Acoust. Soc. Am. 122 (2007) 280–290.
[13] A. Iserles, S. Norsett, From high oscillation to rapid approximation I: Modified Fourier expansions, IMA J. Numer. Anal. 28 (2008) 862–887.
[14] D. Huybrechs, A. Iserles, S. Norsett, From high oscillation to rapid approximation IV: Accelerating convergence, IMA J. Numer. Anal. 31 (2011) 442–468.
[15] B. Adcock, Convergence acceleration of modified Fourier series in one or more dimensions, Math. Comp. 80 (2011) 225–261.
[16] C. Hazard, E. Lunéville, An improved multimodal approach for non-uniform acoustic waveguides, IMA J. Appl. Math. 73 (2008) 668–690.
[17] V. Pagneux, Multimodal admittance method in waveguides and singularity behavior at high frequency, J. Comput. Appl. Math. 234 (2010) 1834–1841.
[18] S.W. Rienstra, A classification of duct modes based on surface waves, Wave Motion 37 (2003) 119–135.